



Computation of Aerodynamic Load(s) Induced Stresses on Horizontal Axis Wind Turbine Rotor Blade with Distinct Configurations

Ekom Mike ETUK¹, Emem Okon IKPE², Aniekan Essienubong IKPE^{3*}

¹University of Benin, Department of Production Engineering, Benin City, PMB 1154, Nigeria

²Akwa Ibom State Polytechnic, Department of Science Technology, Ikot Osurua, PMB 1200, Nigeria

³University of Benin, Department of Mechanical Engineering, Benin City, PMB 1154, Nigeria.

Keywords	Abstract
Wind Turbine	The kinetics of wind turbine blade operation in a wind field domain is complex, as rotor blades in attempt to overcome the aerodynamic loads (drag and wake) counteracting the motion of the blade undergo deflections due to induced stresses. In this study, blade tip deflections and induced stresses on NACA 4610 horizontal wind turbine airfoil were investigated at different wind speeds for three (3) different blade configurations (hollow with spar, hollow no spar and solid configuration), to determine rotor configuration with optimum service performance. Using QBlade v0.8, aerodynamic load induced stresses were computed for normal and tangential loads at wind speeds of 2, 4, 6 and 8 m/s for three horizontal axis wind turbine rotor blade configurations namely: hollow with spar, hollow no spar and the solid configuration. The blade tip deflections as well as the resultant fatigue stress for both x and z axis at wind speeds of 2, 4 6 and 8 m/s were observed to increase proportionately with the wind speeds. Within a wind speed of 2-8 m/s, tip deflections increased from 5.8203e-03 to 0.2873 mm and 0.5700 to 1.7347 mm on the x and z axis, while the resultant fatigue stresses also increased from 2.77 to 8.19 MPa for the hollow blade configured with spar. The tip deflections also increased from 5.86483e-03 to 0.2971 mm and 0.589 to 1.7900 mm on the x and z axis with resultant fatigue stresses from 2.88 to 8.54 MPa for hollow blade configured with no spar. Similarly for the solid blade configuration at wind speed of 2-8 m/s, the tip deflections increased from 3.530097e-03 to 0.180601 mm and 0.363439 to 1.09563 mm with resultant fatigue stresses also increasing from 1.91 to 5.55 MPa. Maximum von-Mises stresses recorded along the blade radius occurred at the mid-section (1.2 m), and were 5554030, 81898880 and 8536480 Pa for solid, hollow with spar and hollow with no spar. The solid blade configuration produced the lowest blade tip deflections, fatigue stresses and von-Mises stresses, indicating that it has a higher load bearing capacity than hollow blade with spar and hollow blade with no spar.
Spar	
Tip Deflection	
von-Mises Stress	
Blade Configurations	
Aerodynamic Loads	

Cite

Etuk, E. M., Ikpe, E. O., & Ikpe, A. E. (2021). Computation of Aerodynamic Load(s) Induced Stresses on Horizontal Axis Wind Turbine Rotor Blade with Distinct Configurations. *GU J Sci, Part A, 8(3)*, 327-338.

Author ID (ORCID Number)

E. M. Etuk, 0000-0002-1866-9349
 E. O. Ikpe, 0000-0001-8093-9904
 A. E. Ikpe, 0000-0001-9069-9676

Article Process

Submission Date 07.07.2021
Revision Date 14.07.2021
Accepted Date 29.07.2021
Published Date 29.07.2021

1. INTRODUCTION

The wind speed in Nigeria varies from 2 m/s to 9.5 m/s, making Nigeria one of the countries in the world with low wind speed (Oyewole & Aro, 2018). For aerodynamic purpose, rotor blade materials such as the wind turbine must possess high fatigue strength, stiffness and low density for optimum performance (Ikpe et al., 2016), even in low wind speed regions. El Khchine et al. (2019) demonstrated that horizontal wind turbine can function in low wind speed regions compared to the vertical axis wind turbine. Wind turbine rotor blades are subjected to high fatigue cycle and vibrational frequency that can expose the blades to failure during rotation if proper monitoring and control devices are not installed. In addition, it is subjected to a wide range of loads such as flapping, tension and compression, twisting etc. all induced by the rotational movement and variable

*Corresponding Author, e-mail: aniekan.ikpe@eng.uniben.edu

aerodynamic loads (Hogg, 2010). Lee et al. (2015) conducted an experiment on the downtime and maintenance cost of a wind turbine, and found that, the rotor blade incurs 30% of the total cost and as well contribute to 34% of the wind turbine downtime. Sutherland (2000) placed more emphasis on glass fibre as a better wind turbine blade material due to its high-strength-to-weight ratio, high stiffness and its ability to adjust to the in-service loading condition of the rotor blade. Okokpujie et al. (2020) employed AHP and TOPSIS multi-criteria decision method in the selection of four (4) suitable horizontal wind turbine blade materials. Performance scores for these materials via TOPSIS techniques were: 78% for aluminium alloy, 43% for stainless steel, 67% for glass fibre and 25% for mild steel, indicating aluminium alloy as the most suitable, followed by glass fibre. Etuk et al. (2020) examined the normal, radial, axial and tangential loading cycles undergone by wind turbine rotor blades and their effects on the displacement of the blade structure using QBlade finite element sub module. Geometry of the deformed blades were characterized by twisting and bending configuration at maximum strain deformation at frequencies up to 200 Hz. From the deflection values obtained, it was found that normal loading cycle would cause the highest level of structural damage on the rotor blade followed by radial, axial and tangential loading. In this study, induced stresses and tip deflection caused by aerodynamic loads were investigated on three (3) wind turbine rotor blade configuration to determine the optimum configuration for best performance.

2. MATERIAL AND METHOD

This Study was carried out using three horizontal wind turbine blade configurations as shown in Figure 1. The loading data was imported from a previously simulated turbine that uses the same rotor. For the structural blade design module, a simple structural model for the blade was defined inside the Structural Blade Design and Analysis tab in QBlade v0.8. The model was defined and simulated using isotropic material properties only. After defining the structural model and the Save button was clicked, the sectional blade properties were automatically computed. Static loading simulation was set up from the Static Loading/Deflection tab where the blade tip deflections as well as the resultant fatigue stress for both x and z axis of the blade were computed for the three (3) blade configurations (hollow with spar, hollow no spar and the solid configuration) at various windspeeds (2, 4, 6 and 8 m/s). After clicking the Save button, the static deflection and blade surface stresses (von Mises) were computed and displayed in the 3D Views. At this stage, the structural properties as well as the results of the loading simulation were plotted in graphs, by changing to Graph View in the toolbar.

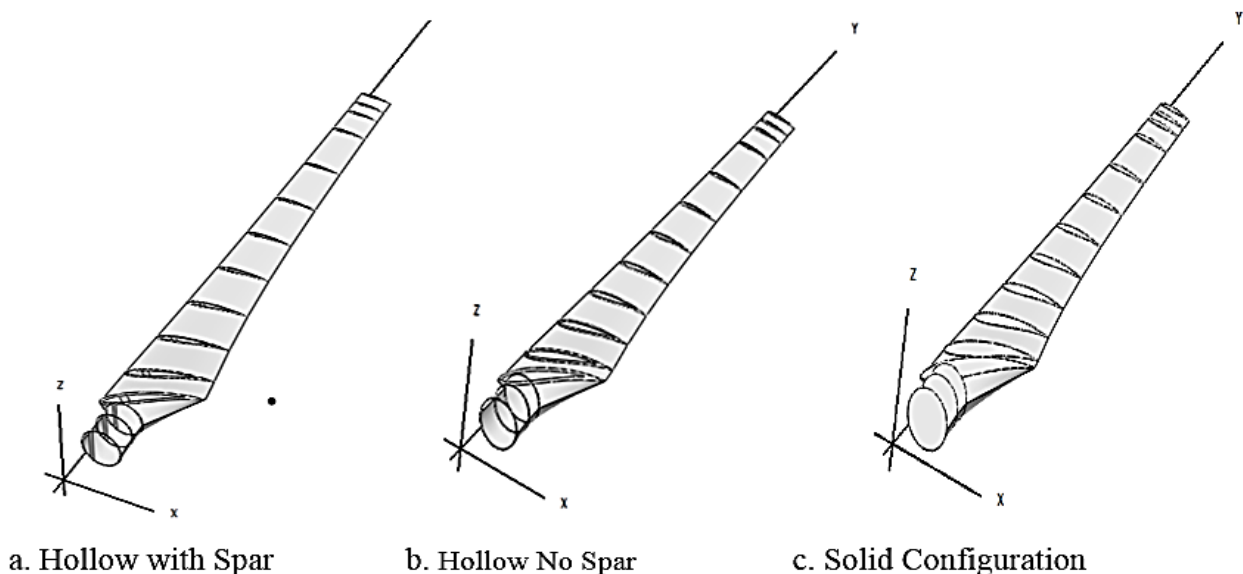


Figure 1. Illustration of the Rotor Blade Section, a) Hollow with Spar, b) Hollow No Spar, c) Solid Configuration

Figure 1 represents typical rotor blade configurations for horizontal wind turbine application. It can be observed in the above rotor blade configurations that some blades are configured with a hollow pattern reinforced with spar, some are configured with just a hollow pattern with no spar while some are configured without spar and hollow pattern. The hollow pattern is simply a configuration in which a centre hole or trench

is made at the mid-section of the blade. This is sometimes applicable to high density rotor blades where the mid-section are made hollow in order to reduce the blade density. In such case, the trench can extend fully or partially along the length (i.e., span-wise direction) of the blade.

The term “spar” is a beam-like structural member that supports the ribs in an airfoil, aircraft wing or wind rotor blades, and running span-wise at right angles to the blade leading edge. In other words, spars which serves as a reinforcing members of a wind turbine rotor blade increases the structural strength and stiffness of the blade to prevent tower strikes in the event of sudden wind gusts, forms the structural framework upon which reduction in axial fatigue, improvement of compressive strain, buckling resistance as well as resistance to gravitational and aerodynamic loads are well assured. Spars are usually “L or T” shaped member installed within the hollow section of the rotor blade. It consist of upper and lower members known as spar caps and vertical sheet members known as shear webs that span the distance between the spar caps of which the spar caps are welded or riveted to the top and bottom of the vertical member to prevent buckling.

The third rotor blade configuration as shown in Figure 1 is the solid configuration which neither has spars nor hole in the mid-section of the blade. The solid blade in this case is densely rigid with no internal holds, solid in cross section with both interior and exterior part uniformly filled with the same material. Like every other rotor blades, the leading and trailing edges are properly streamlined to meet aerodynamic specifications for wind turbine rotor blades. Material and blade properties of the wind turbine rotor blade are presented in Table 1.

Table 1. Material Properties of the 6000 Series Aluminium Rotor Blade

Properties	Shell Material specifications	Internal Material specifications
	6000 Series Aluminium	Polyurethane 20GF 6SD
Density (kg/m ³)	2740	1360
Elastic Modulus (MPa)	7e+04	1.72e+03
Mass (kg)	Hollow with Spar: 13.2465 Hollow no Spar: 12.1003 solid: 31.535	
Section No.	Rotational Speed	119(1/min)
	Shell Thickness (m)	Spar Thickness (m)
1	0.00320	0.01280
2	0.0030	0.01200
3	0.0030	0.01200
4	0.00961	0.03844
5	0.00773	0.03092
6	0.00606	0.02423
7	0.00495	0.01981
8	0.00418	0.01671
9	0.00361	0.01444
10	0.00317	0.01269
11	0.00283	0.01132
12	0.00255	0.01021
13	0.00243	0.00974
14	0.00238	0.00952
15	0.00233	0.00930

QBlade is a Blade Element Moment Method (BEM), Double Multiple Streamtube (DMS) and nonlinear lifting line theory (LLT) design and simulation software for vertical and horizontal axis wind turbine. QBlade incorporates a number of tools such as QFEM to setup and simulate the internal blade structure and perform structural blade design, modal analysis, static deflection as well as stress analysis. QBlade v0.8 was employed in the computation of aerodynamic load(s) acting tangentially and normally along the blade length for different blade configurations and using Finite Element Method (FEM) to evaluate the induced stresses and tip deflections at x, y and z axis. This was done in order to determine the most suitable blade configuration that can withstand structural failure due to aerodynamic loads/forces from the wind. The respective chord lengths and angle of twist of each section is shown in Figure 2. The total length of the blade was 2.2m, total number of sections was 15 while the number of blades employed in the simulation process was 3. The blade was divided into 15 sections the first three sections had the circular foil applied at the blade section while the remaining 12 sections had NACA 4610 airfoil applied on them. The blade geometry/root coordinates is presented in Figure 2. Loading data was imported from a previously simulated turbine that uses the same rotor. In the structural blade design module, a simple structural model was defined for the rotor blade inside the Structural Blade Design/Modal Analysis tab. The model was defined and simulated using isotropic material properties only.

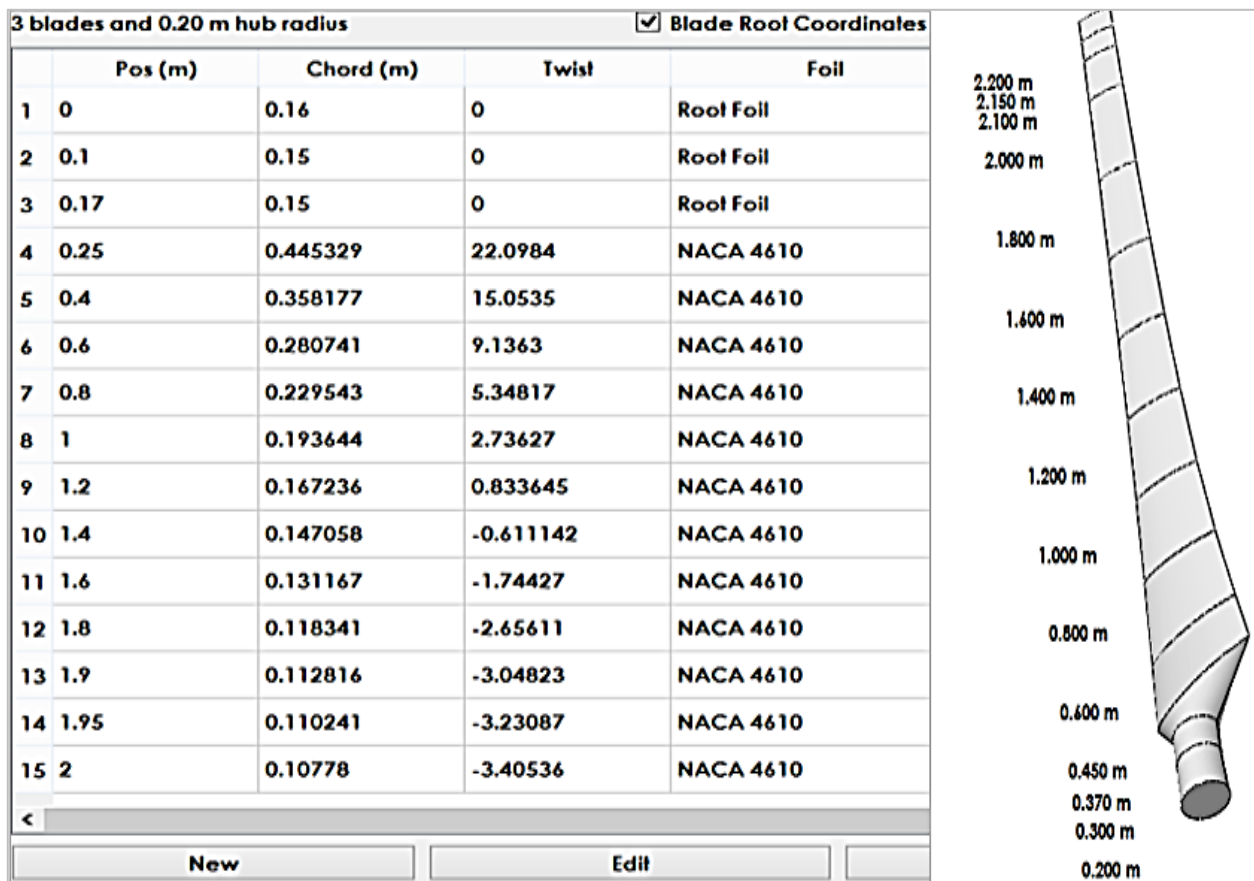


Figure 2. Blade Geometry/Root Coordinates

3. RESULTS AND DISCUSSION

When the direction of wind flows along a cambered airfoil/wind rotor blade which has some degree of curvature, the wind velocity and acceleration continues to change along the blade radius, producing aerodynamic forces that acts on the blade as the wind speed changes. Two (2) components of force can be taken at any given point on the curved blade. One component of force is normal to the tangent or towards the centre of curvature of the rotor blade. This component is known as the normal force acting at that point. Normal loading or forces are those forces acting perpendicularly to the direction of motion. In other words, normal component of force does not change the magnitude of the flow velocity, but changes the direction of velocity at that point. Values obtained for normal loading acting along the turbine rotor blade length at different wind

speeds are graphically represented in Figure 3. The plot indicates that the normal loads increase as the wind speed and the blade length increases

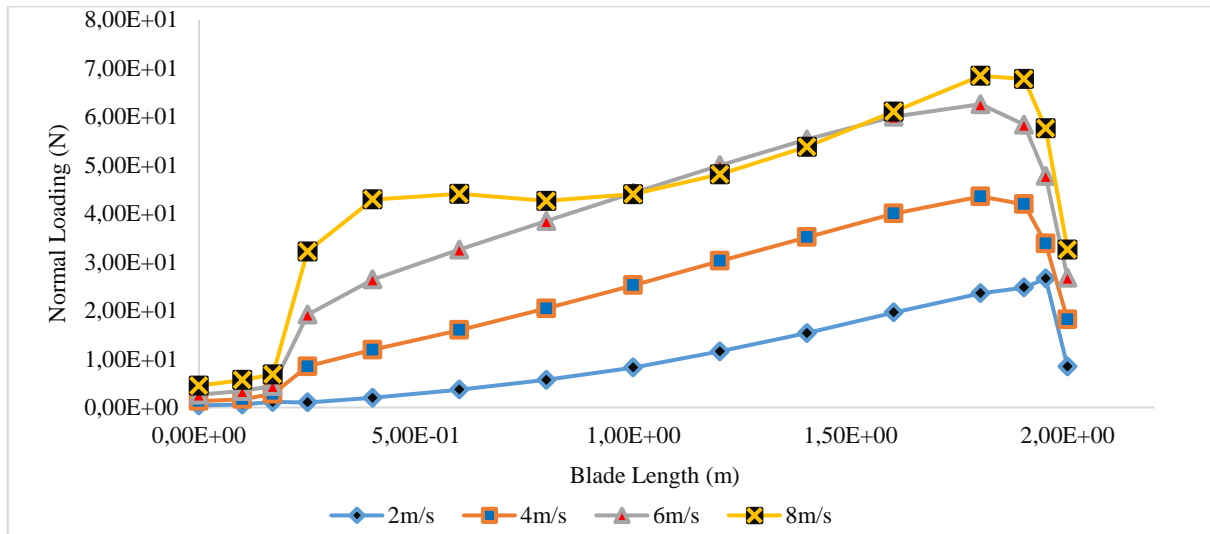


Figure 3. Plot of Normal Loading (N) Acting along Blade Length

The other component of force is in the direction of tangent to the blade at a given point. This component is known as the tangential force acting at that point. Tangential loading or forces are those forces acting along the direction of motion. In other words, the said tangential force does not change the direction of motion but changes the velocity magnitude. Values obtained for tangential loading acting along the turbine rotor blade length at different wind speeds are graphically represented in Figure 4. The plot indicates that the tangential loads increase as the wind speed and the blade length increases. This is because the trailing edge of the blade towards the tip becomes narrower and more streamlined, as such overcomes drag and wake forces easily at higher wind speeds.

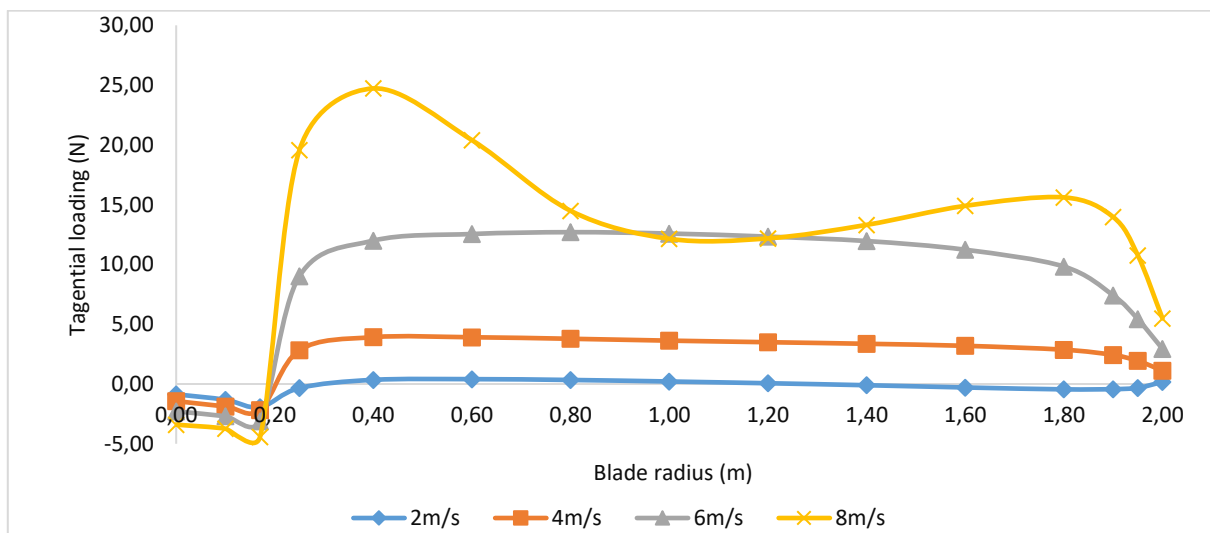


Figure 4. Plot of Tangential Loading on Blade Length at Different Wind speeds

3.1. Deflection and Fatigue Results for Hollow with Spar

Figure 5 indicate the stresses and tip deflections along x and z axis of the rotor blade at wind speeds of 2, 4, 6 and 8m/s respectively for hollow blade with spar. Some level of curiosity may be arouse as to why the tip deflection was determined for only x and z axis without considering the y axis. As presented in the blade configurations in Figure 1, y-axis is towards the direction of the blade length and it is not possible for the blade to elongate in that direction because it is constrained not to. As discussed earlier in Figure 1, the blade configuration with hole and spar is designed as a reinforcement for the blade to withstand more aerodynamic

loads than the hollow blade without spar. Ikpe et al. (2017a) suggested that engineering components subjected to high or low loading conditions be reinforced for adequate stiffness, fracture toughness and yield strength at critical operating conditions. The simulation for the hollow blade configured with spar in this case was carried out at a wind speed of 2m/s, 4m/s, 6m/s and 8m/s and the corresponding tip deflections on the x-axis were 5.8203e-3, 7.56706e-02, 0.212186 and 0.2873 mm while the corresponding tip deflections on the z-axis were 0.5700, 1.08238, 1.61323 and 1.7347 mm as shown in Figure 5. The resultant fatigue stresses of 2.77, 5.00, 7.28 and 8.19 MPa for the same set of wind speeds as shown in Figure 5. From the aforementioned set of results obtained for hollow blade with spar, it is obvious that an increase in the tip deflection of both x and z-axis of the rotor blade led to increase in the resultant fatigue stress for each wind speed that the blade operates under.

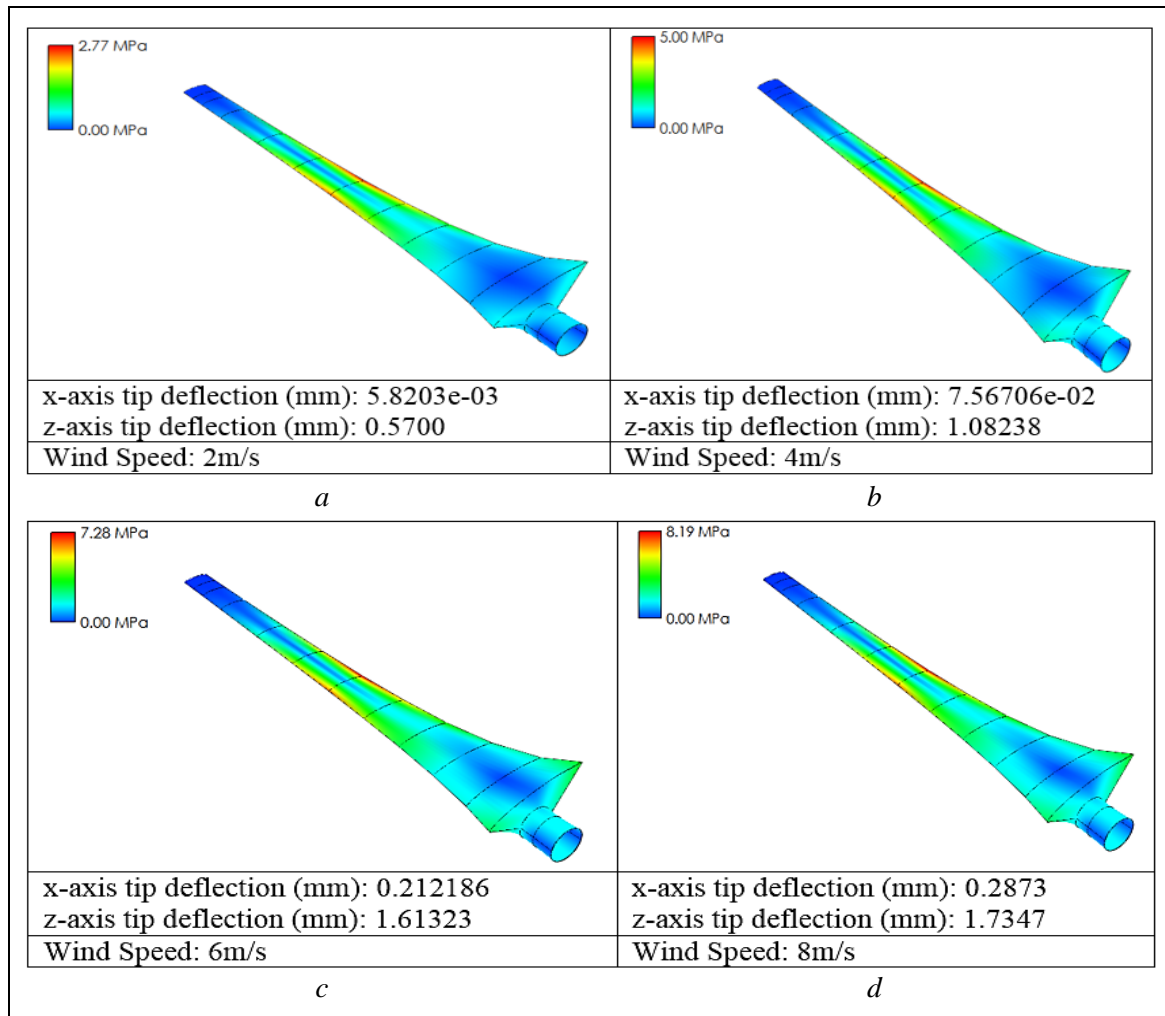


Figure 5. x and z-axis Tip Deflection at Wind Speed of a) 2m/s, b) 4m/s, c) 6m/s, d) 8m/s

3.2. Deflection and Fatigue for Hollow Blade No Spar

Figure 6 indicate the stresses and tip deflections along x and z axis of the rotor blade at wind speeds of 2, 4, 6 and 8m/s respectively for hollow blade with no spar. As discussed earlier in Figure 1, such blade configuration may have limitations due the internal hole which may serve as a vacuum/voids that prevents the blade to perform optimally or maintain its structural integrity in events of high impact loads on them. Furthermore, such blade configuration may also fail to meet its design life due stress fatigue which can envelope around the hollow region and eventually give way due to lack of reinforcement with spars to enable it withstand high impact loads of prolong fatigue cycles at extreme operating conditions. The simulation for the hollow blade configured with no spar was carried out at similar wind speeds of 2, 4, 6 and 8m/s, and the corresponding tip deflections on the x-axis were 5.86483e-3, 7.806e-02, 0.21957 and 0.2971 mm while the corresponding tip deflections on the z-axis were 0.589, 1.11707, 1.66475 and 1.7900 mm as presented in Figure 6. The resultant

fatigue stresses of 2.88, 5.21, 7.59 and 8.54 MPa for the same set of wind speeds as presented in Figure 6. From the aforementioned set of results obtained for hollow blade with no spar, the trend of the tip deflection values for both x and z-axis of the rotor blade increases proportionately with the wind speed and this subsequently led to increase in the resultant fatigue stress for each wind speed as was in the previous case of hollow blade configuration with spar. From the two scenarios, blade tip deflection in both axis as well as the resultant fatigue stresses for hollow blade configuration with spar were lower than hollow blade configuration with no spar, indicating that hollow blade with spar may provide a higher structural strength than hollow blade with no spar.

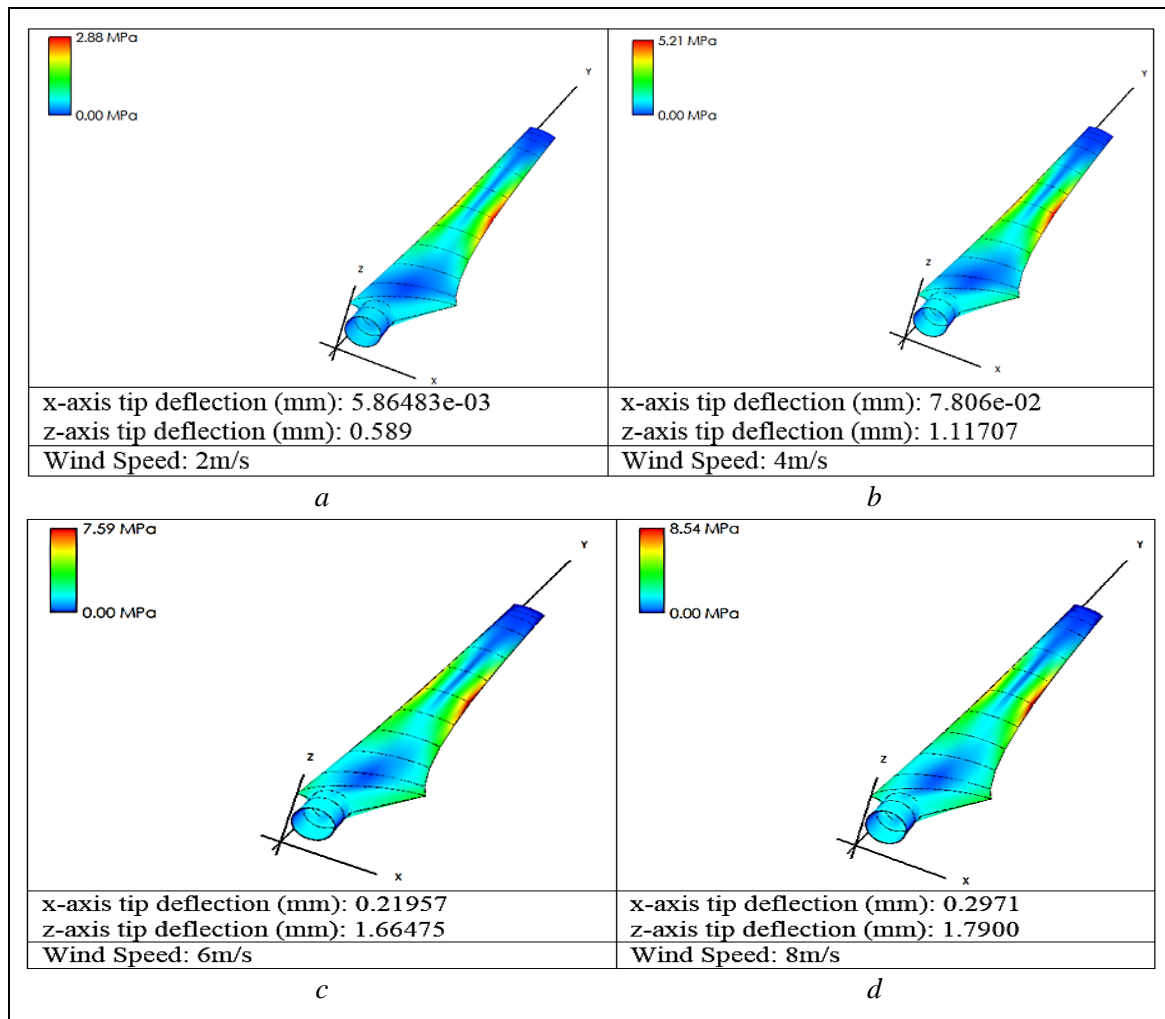


Figure 6. x and z-axis Tip Deflection at Wind Speed of a) 2m/s, b) 4m/s, c) 6m/s, d) 8m/s

3.3. Deflection and Fatigue for Solid Blade

Figure 7 indicate the stresses and tip deflections along x and z axis of the rotor blade at wind speeds of 2, 4, 6 and 8m/s respectively for solid blade configuration. The simulation for the solid blade configured with no spar and no hole at the internal mid-section was carried out at similar wind speeds of 2, 4, 6 and 8m/s, and the corresponding tip deflections on the x-axis were 3.53097e-03, 4.728e-02, 0.133085 and 0.180601 mm while the corresponding tip deflections on the z-axis were 0.363439, 0.685309, 1.01855 and 1.09563 mm as shown in Figure 7. The resultant fatigue stresses of 1.91, 3.41, 4.92 and 5.55 MPa for the same set of wind speeds as shown in Figure 7. From the aforementioned set of results obtained for the solid blade configuration in this study, the trend of tip deflection values for both x and z-axis of the rotor blade increases as the wind speed also increase and this also influenced the resultant fatigue stress for each wind speed, as it also increased. Results of the simulation carried out on the solid blade configuration resulted in lower tip deflection for both axis as well as the resultant fatigue stresses than the blade tip deflections and resultant fatigue stresses obtained for

hollow blade with and without spar. This implies that solid rotor blade in wind turbine application can offer a higher structural strength and less possibility of failure in its service condition.

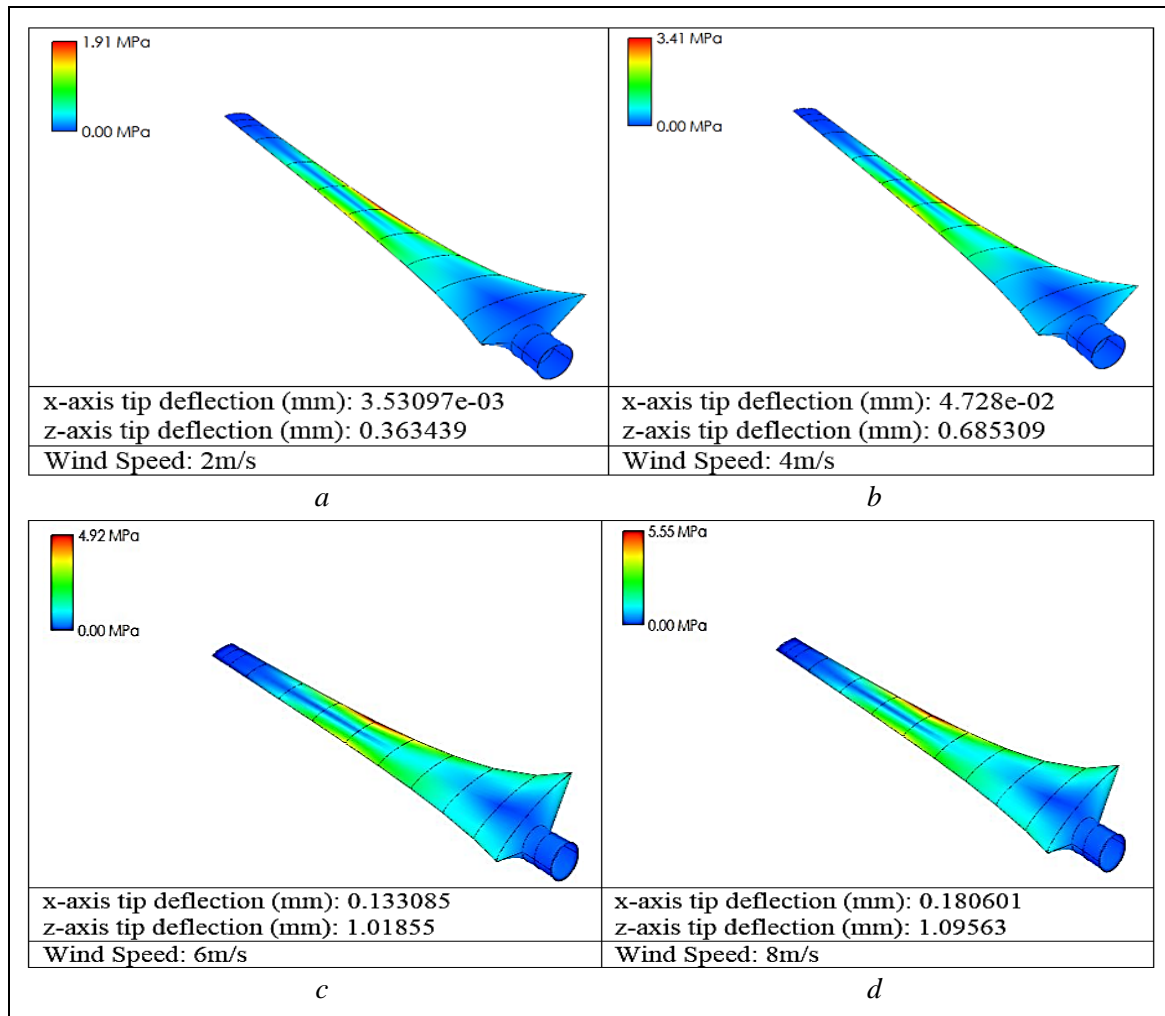


Figure 7. *x* and *z*-axis Tip Deflection at Wind Speed of **a)** 2m/s, **b)** 4m/s, **c)** 6m/s, **d)** 8m/s

From the colour distribution patterns on the simulated blade configuration shown in Figures 5-7, red colour indicates the area with the highest fatigue stress concentration on the rotor blade, royal blue indicates the minimum fatigue stress on the blade or the state in which the blade is not subjected to fatigue loads, sky blue indicates the state at which the blade begins to respond to stress due to fatigue cycles, aqua (SVG) blue indicates further responses of the blade material to fatigue stresses lower than those signified by sky blue (Owunna et al., 2018). The light green, yellow and orange colour profiles signifies fatigue stresses higher than those signified by the blue colour profile but lower than those signified by red colour profile. From the rotor blade simulation profiles represented in Figure 5-7, highest fatigue stresses is observed to occur at the mid-section of the blade for each wind speed. This indicates that the rotor blade is prone to failure at a much higher fatigue stress value in its mid-section. Fatigue stress in this context occurs when the rotor blade undergoes cyclic repeated load which may translate into cracks depending on the extent of initial damage and the cyclic loads afterwards. From the standpoint of fracture mechanics, the initial damage may occur on the blade material after its properties have been depleted due to exposure to its in-service loading conditions. During a large number of loading cycles, the damage develops on a microscopic level and grows until a microscopic crack is formed. The microscopic crack grows further as the loading cycle progresses until it reaches a critical length where the cracked blade material can no longer sustain the peak load and fails. Such a failure depends on whether the material is ductile or brittle as well as the degree of peak load. The aforementioned discussions on the three blade configurations simulated in this study is further buttressed in the graphical representation of rotor blade tip deflections shown in Figures 8-9 which clearly reveals that the blade tip deflection increases as the wind speed increase.

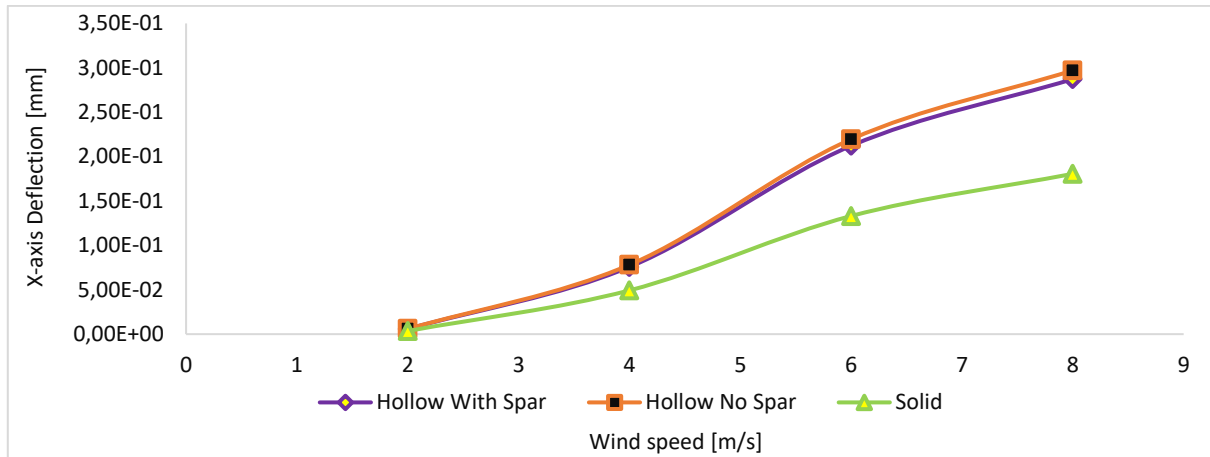


Figure 8. Plot of X-axis Tip Deflection against Wind speed for Various Blade Types

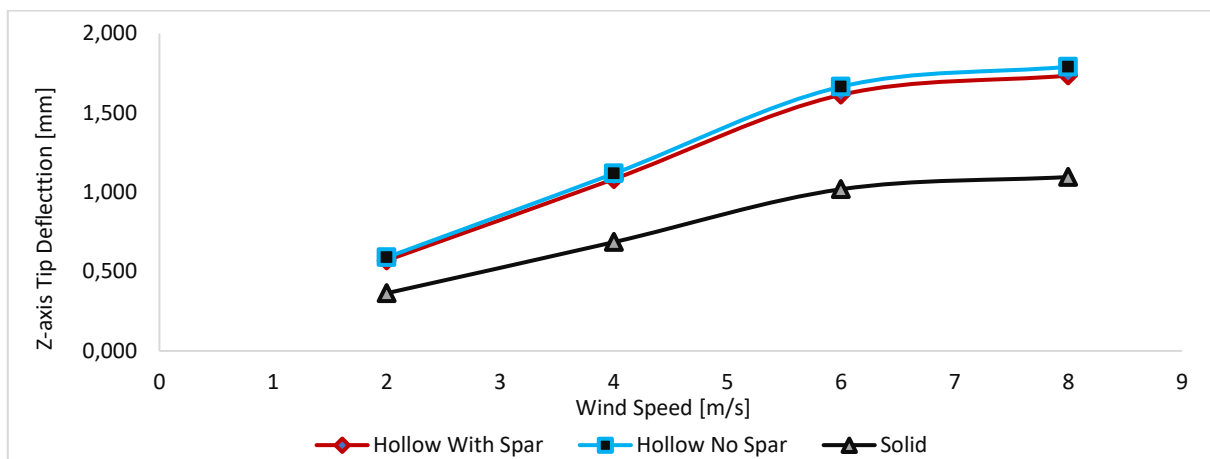


Figure 9. Plot of Z-axis Tip Deflection against Wind speed for Various Blade Types

3.4. von-Mises Stress Results for Blade Configurations

The von-Mises yield criterion also known as maximum distortion criterion relates to plasticity theory which states that yielding begin in ductile materials (such as 6000 Series Aluminium used in this study) when the second invariant of deviatoric stress attains a critical value (Ikpe et al., 2017b; Owunna & Ikpe, 2019). It can also be employed in predicting yielding of a material under variable loads. Under such condition, the material is considered to have started yielding when the von-Mises stress is close to or reaches the yield strength of the material and considered to have failed when the von-Mises stress exceeds the material yield strength (Efe-Ononeme et al., 2018). However, if the von-mises stress value is much less than the material’s yield strength, it can be considered that the material still has the strength to withstand additional forces/loads before failure. This relates to the theory behind elasticity of materials which state that a given material under its service condition can accommodate additional loads/forces provided its elastic limit is not exceeded (Ebunilo et al., 2016; Ikpe & Owunna, 2017). Figures 10-13 represent plots of maximum von-Mises stress in in Pascal (Pa) along the blade radius at 2, 4, 6, and 8 m/s for the three (3) rotor blade configurations considered in this study. It can be observed that maximum von-Mises stress along the blade at 2 m/s is 2771490 Pa for hollow blade configuration with spar, 2880810 Pa for hollow blade configuration with no spar and 1914440 Pa for the solid blade configuration as shown in Figure 10. Maximum von-Mises stress along the blade at 4 m/s is 5001160 Pa for hollow blade configuration with spar, 5208880 Pa for hollow blade configuration with no spar and 3410090 Pa for the solid blade configuration as shown in Figure 11. Maximum von-Mises stress along the blade at 6 m/s is 7279370 Pa for hollow blade configuration with spar, 7592530 Pa for hollow blade configuration with no spar and 4917400 Pa for the solid blade configuration as shown in Figure 12. Finally for maximum von-Mises stress along the blade at 8 m/s, 8189880 Pa is observed for hollow blade configuration with spar, 8536480 Pa for hollow blade configuration with no spar and 5554030 Pa for the solid blade configuration as shown in Figure 13. Considering the von-Mises failure criterion discussed earlier, the maximum von-Mises

stress value among all the wind speeds considered in this study occurred at 8 m/s which were 8536480 Pa (approximately 8.53 MPa) for hollow blade configuration with no spar, 8189880 Pa (approximately 8.18 MPa) and 5554030 Pa (approximately 5.55 MPa) for the solid blade configuration. These von-Mises stress values has not exceeded the aluminium blade material yield strength of 2.76×10^8 Pa (approximately 276 MPa), indicating that the material has not failed. The difference between the maximum von-Mises and the yield strength of the material indicates whether or not the blade material still has the capacity to withstand more loads before yielding. Highest values obtained for maximum von-Mises stress on the rotor blade at various wind speeds considered in this study is observed to occur at 1.2 m of the blade length. Since the loads acting on the blade are not point loads and therefore distributed along the edge, highest values obtained for maximum von-Mises stress on the rotor blade at various wind speeds in this study is observed to occur at the mid-section of the rotor between 1 and 1.4 m of the blade length as graphically illustrated in Figure 10-13. This implies that the mid-section of the blade is exposed to the highest service loads, and that failure will most like occur along this section depending whether the von-Mises stress exceeds the blade material yield strength or not. Wind turbine blades are composed of two faces (the suction face and the pressure face), bound together and stiffened either by one or more integral (shear) webs connecting the upper and lower section of the blade shell or by a box beam (box spar with shell fairings) (Brøndsted & Nijssen, 2013). The shells are adhesively joined together to the spars. The flapwise load is as a result of the wind pressure while the edgewise load is due to gravitational forces and torque load acting on the blade. The flapwise bending is resisted by the spar, internal webs or spar inside the blade, while the edges of the profile carry the edgewise bending. From the point of loads on materials, one of the main laminates in the main spar is subjected to cyclic tension-tension loads (pressure side) while the other (suction side) is subjected to cyclic compression-compression loads. The laminates at the leading and trailing edges that carry the bending moments related to the gravitation loads are subjected to tension-compression loads (Mishnaevsky et al., 2017; Etuk et al., 2021).

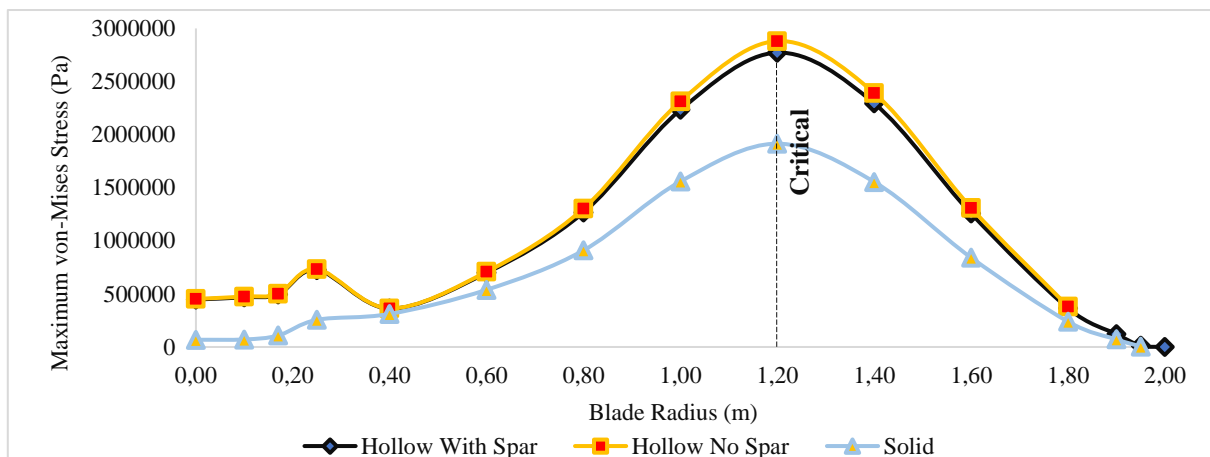


Figure 10. Plot of Maximum von-Mises Stress along Blade @ 2m/s

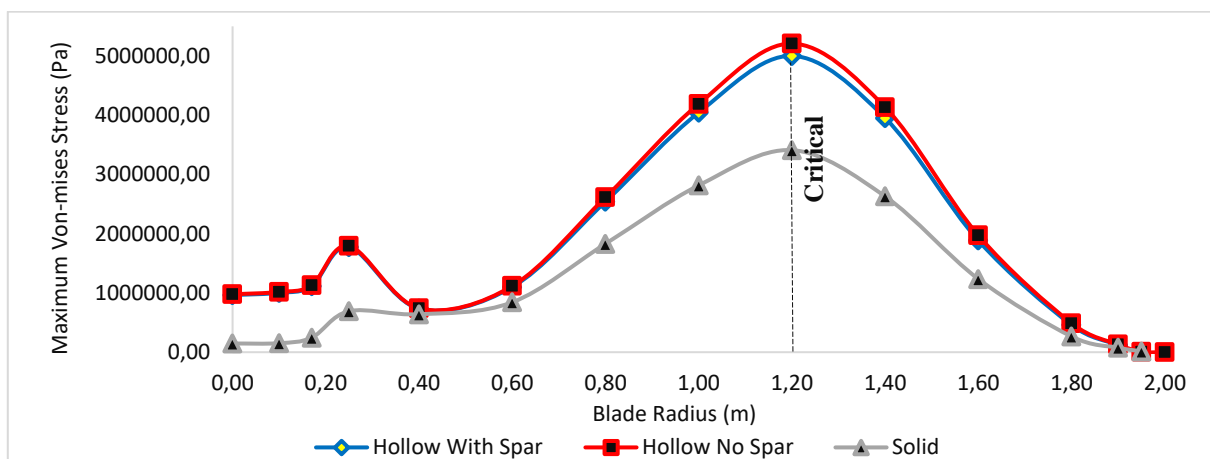


Figure 11. Maximum von-Mises Stress along Blade @ 4m/s

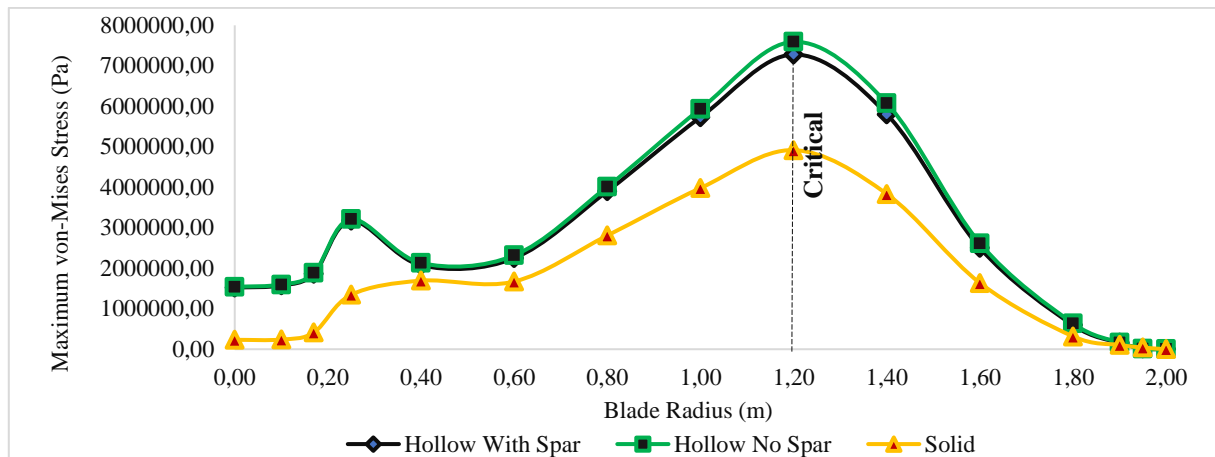


Figure 12. Plot of Maximum von-Mises Stress along Blade @ 6m/s

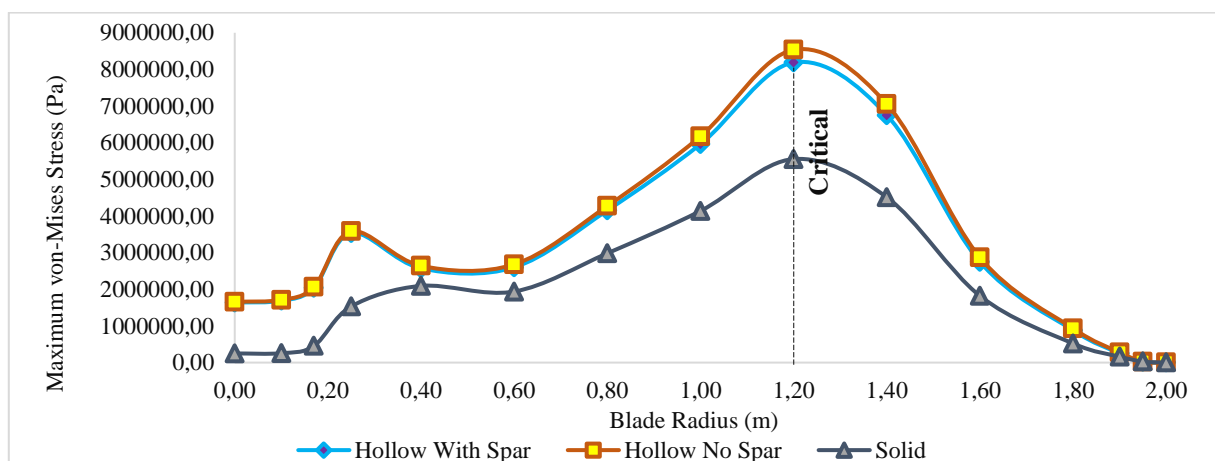


Figure 13. Plot of Maximum von-Mises Stress along Blade @ 8m/s

4. CONCLUSION

In this study, the in-service load(s) induced stresses on horizontal axis wind turbine rotor blade was successfully computed for three (3) blade configurations (hollow with spar, hollow with no spar and solid). The highest fatigue stress was observed to occur at the mid length of the rotor blade. The minimum stress was at the blade tip where no stress is present due to its streamlined geometry. Compared to the hollow blade configuration with spar and without spar, the solid blade though slightly heavier, was more rigid and compact, with increased load bearing capacity and ability to withstand fatigue stress. Both the fatigue stresses and von-Mises stresses were observed to increase proportionately with the wind speed, implying that the wind rotor blade material is susceptible to deformation and failure at increasing wind speed, aerodynamic forces and in-service loading conditions.

CONFLICT OF INTEREST

We the authors of this manuscript have declared that there is no conflict of interest associated with the publication of this paper.

REFERENCES

- Brøndsted, P. & Nijssen, R. (2013). *Advances in Wind Turbine Blade Design and Materials*. Woodhead Publishing, Oxford, UK, 484 p.
- Ebunilo, P. O., Ikpe, A. E. & Owunna, I. (2016). Determining the Accuracy of Finite Element Analysis when Compared to Experimental Approach for Measuring Stress and Strain on a Connecting Rod Subjected to Variable Loads. *Journal of Robotics, Computer Vision and Graphics*, 1(1), 12-20.

- Efe-Ononeme, O. E., Ikpe, A. E. & Ariavie, G. O. (2018). Thermo-Structural Analysis of First Stage Gas Turbine Rotor Blade Materials for Optimum Service Performance. *International Journal of Engineering and Applied Sciences*, 10(2), 118-130.
- El Khchine, Y., Sriti, M. & Elyamani, N. E. (2019). Evaluation of Wind Energy Potential and Trends in Morocco. *Heliyon*, 6(6), 18-30.
- Etuk, E. M., Ikpe, A. E. & Adoh, U. A. (2020). Design and Analysis of Displacement Models for Modular Horizontal Wind Turbine Blade Structure. *Nigerian Journal of Technology*, 39(1), 121-130.
- Etuk, E. M., Ikpe, A. E. & Ndon, A. E. (2021). Modal Analysis of Horizontal Axis Wind Turbine Rotor Blade with Distinct Configurations under Aerodynamic Loading Cycle. *Gazi University Journal of Science Part A: Engineering and Innovation*, 8(1), 81-93.
- Hogg, P. (2010). Wind Turbine Blade Materials. SUPERGEN Wind Phase 1 Final Assemble, University of Loughborough, March 25th, 2010. Engineering and Physical Science Research Council.
- Ikpe, A. E., Owunna, I., Ebunilo, P. O. & Ikpe, E. (2016). Material Selection for High Pressure (HP) Turbine Blade of Conventional Turbojet Engines. *American Journal of Mechanical and Industrial Engineering*, 1(1), 1-9.
- Ikpe, A. E., Orhororo, E. K. & Gobir, A. (2017a). Design and Reinforcement of a B-Pillar for Occupants Safety in Conventional Vehicle Applications. *International Journal of Mathematical, Engineering and Management Sciences*, 2(1), 37-52.
- Ikpe, A. E., Owunna, I. B. & Satope, P. (2017b). Design optimization of a B-pillar for crashworthiness of vehicle side impact. *Journal of Mechanical Engineering and Sciences*, 11(2), 2693-2710.
- Ikpe, A. E. & Owunna, I. (2017). Design of Vehicle Compression Springs for Optimum Performance in their Service Condition. *International Journal of Engineering Research in Africa*, 33, 22-34.
- Lee, J. K., Park, J. Y., Oh, K. Y., Ju, S. H. & Lee, J. S. (2015). Transformation Algorithm of Wind Turbine Blade Moment Signals for Blade Condition Monitoring. *Renewable Energy*, 79, 209-218.
- Mishnaevsky, L., Branner, K., Petersen, H. N., Beauson, J., McGugan, M & Sørensen, B. F. (2017). Materials for Wind Turbine Blades: An Overview. *Materials*, 10(1285), 1-24.
- Okokpujie, I. P., Okonkwo, U. C., Bolu, C. A., Ohunakin, O. S., Agboola, M. G. & Atayero, A. A. (2020). Implementation of Multi-criteria Decision Method for Selection of Suitable Material for Development of Horizontal Wind Turbine Blade for Sustainable Energy Generation. *Heliyon*, 6, e03142.
- Owunna, I. B. & Ikpe, A. E. (2019). Evaluation of induced residual stresses on AISI 1020 low carbon steel plate from experimental and FEM approach during TIG welding process. *Journal of Mechanical Engineering and Sciences*, 13(1), 4415-4433.
- Owunna, I., Ikpe, A. E. & Achebo, J. I. (2018). Temperature and Time Dependent Analysis of Tungsten Inert Gas Welding of Low Carbon Steel Plate using Goldak Model Heat Source. *Journal of Applied Science and Environmental Management*, 22(11), 1719-1725.
- Oyewole, J. A. & Aro, T. O. (2018). Wind Speed Pattern in Nigeria (A Case Study of some Coastal and Inland Areas). *Journal of Applied Science and Environmental Management*, 22(1), 119-123.
- Sutherland, H. J. (2000). A summary of the Fatigue Properties of Wind Turbine Materials. *Wind Energy*, 3, 1-34.